

Lagrangian Velocity Correlations and Absolute Dispersion in the Midlatitude Troposphere

Jai Sukhatme

Advanced Study Program, National Center for Atmospheric Research, Boulder, CO

(July 22, 2018)

Employing daily wind data from the ECMWF, we perform passive particle advection to estimate the Lagrangian velocity correlation functions (LVCF) associated with the midlatitude tropospheric flow. In particular we decompose the velocity field into time mean and transient (or eddy) components to better understand the nature of the LVCF's. A closely related quantity, the absolute dispersion (AD) is also examined.

Given the anisotropy of the flow, meridional and zonal characteristics are considered separately. The zonal LVCF is seen to be non-exponential. In fact, for intermediate timescales it can either be interpreted as a power law of the form $\tau^{-\alpha}$ with $0 < \alpha < 1$ or as the sum of exponentials with differing timescales - both interpretations being equivalent. More importantly the long time correlations in the zonal flow result in a superdiffusive zonal AD regime. On the other hand, the meridional LVCF decays rapidly to zero. Before approaching zero the meridional LVCF shows a region of negative correlation - a consequence of the presence of planetary scale Rossby waves. As a result the meridional AD, apart from showing the classical asymptotic ballistic and diffusive regimes, displays transient subdiffusive behaviour.

I. INTRODUCTION

Being a quantity of fundamental interest in the statistical characterization of a turbulent flow, the Lagrangian velocity correlation function (LVCF) has been the subject of detailed study [1], [2]. Indeed, if we view the midlatitude free troposphere to be in a non-ideal turbulent state [3], [4], it is of natural interest inquire into the nature its LVCF. Similarly, apart from being a measure of transport and its close relation to the LVCF [5], [2], the absolute dispersion (AD) is known to yield information about the structure of the underlying flow [6], [7].

Ofcourse there exist other measures, such as the relative dispersion (or Lyapunov exponents for smooth flows) and finite scale analyses (or finite size Lyapunov exponents), which are a part of the complete statistical characterization of a flow. In particular, finite scale statistics are argued to be useful when the available range of scales is small and there is the possibility of crossover effects from differing regimes [8] ¹. Our approach is slightly different from earlier modelling studies of large scale atmospheric dispersion which employ a Langevin equation, equivalently assuming an exponential LVCF, to parameterize the dispersion process [9], [10] (a discussion of such an approach can be found in [11]). In the present note we will only consider the LVCF and AD, focussing their characterization and complementary nature. Also, we will see the accordance of these statistics with simpler physically relevant systems.

For computational purposes, daily pressure level global T63 (192×96 , 17 levels) resolution wind data from the ECMWF is used as the 3D advecting velocity field. We computed the trajectories

¹I thank Referee A for the discussion of finite scale statistics.

(and record the velocity along these trajectories) of an ensemble of passive particles. The trajectories were computed in latitude, longitude and pressure coordinates by a standard fourth order Runge-Kutta scheme and the velocity fields were interpolated in a linear fashion. Averaging is done with respect to an ensemble (denoted by S) of passive particles which remain in the free troposphere, i.e. particles which escape into the boundary layer or into the stratosphere are excluded from the statistics ².

II. LAGRANGIAN VELOCITY CORRELATION FUNCTIONS

A. Zonal LVCF

Denoting the zonal velocity by $u(\lambda, \phi, p, t)$, the zonal LVCF ($R_u(\tau)$) is defined as

$$R_u(\tau) = \frac{\langle u(\vec{x}(t+\tau)) u(\vec{x}(t)) \rangle_S}{\langle u(\vec{x}(t))^2 \rangle_S} \quad (1)$$

Here $\vec{x}(t)$ represents the trajectory of an individual member of S . To account for the inhomogeneity of the flow and to focus our attention the midlatitudes, S is chosen to comprise of N members located randomly such that they initially satisfy $0^\circ < \lambda(S) < 360^\circ$, $35^\circ \leq \phi(S) \leq 55^\circ$ and $400\text{mb} \leq p(S) \leq 700\text{mb}$, where λ, ϕ, p represent the longitude, latitude and pressure coordinates. Note that no restriction is placed on the trajectories, i.e. the statistics presented are *not conditional* on the particles remaining in the midlatitudes for all times.

As can be seen in the upper panel of Fig. 1, which shows $\log[R_u(\tau)]$ for the winter and summer seasons, the zonal LVCF is clearly non-exponential. This is in agreement with studies on 2D [12] and geostrophic [13] turbulence, but stands in contrast to investigations of 3D turbulence [14], [15]. Further, for intermediate values of τ (i.e. $2 < \tau < 10$ days), it appears that (lower panel of Fig. 1) $R_u(\tau) \sim \tau^{-\alpha}$ with $0 < \alpha < 1$ ($\alpha = 0.32$ and 0.45 for DJF and JJA respectively). The issue of whether the correlation function is indeed a power law is known to be a delicate matter. Indeed any monotonically continuous function, such as the aforementioned power law, can be expressed (over a given range of scales) as the discrete sum of exponentials - see Berglund [16] for definitions and details - a fact which has been elegantly utilized in the analysis of queues in communication networks [17], [18]. Whether the zonal LVCF is the sum of two (or more) Ornstein-Uhlenbeck processes with differing timescales - as is argued to be an effective parameterization of the LVCF in 2D turbulence [12] - or, if it indeed shows power-law scaling is practically undecidable especially if the behaviour is seen over a small range of scales ³. On the other hand, what is certain is the enhancement of the Lagrangian correlation time [6] ($T_u = \int_0^\infty R_u(t) dt$). Indeed, as will be observed, the persistent correlations in the zonal velocity field result in a superdiffusive AD regime.

²Experiments were performed with an initial set of 20,000 and 30,000 particles, no discernable difference in the statistics was noticed in these two situations.

³Comments of Referee B are acknowledged as they provoked a more careful look at this issue.

B. Meridional LVCF

Defined in a manner similar to Eq. (1), but using the meridional component of the velocity field ($v(\lambda, \phi, p, t)$) we compute the meridional LVCF ($R_v(\tau)$). As is seen in Fig. 2, $R_v(\tau)$ decays to zero in one week. Interestingly, we notice a pronounced anticorrelation, i.e. $R_v(\tau) < 0$ before the final $R_v(\tau) \rightarrow 0$ behaviour. On comparison with 2D [12] and geostrophic turbulence [13] we find this feature to be unique to the present situation. This is easily explained when one takes into account the latitudinal restriction imposed by the rotation of the planet [19]. Specifically, in the absence of strong diabatic or frictional effects, the conservation of potential vorticity gives rise to large scale Rossby waves [20]. We argue that the meridional oscillatory motion implied by the Rossby waves is responsible for the aforementioned anticorrelation.

C. Eddy and Time Mean LVCF's

To gain some insight into the connection between the nature of the LVCF's and the structure of the tropospheric flow, we partition the daily data into time mean and transient components. Specifically, the time mean is $\hat{u}(\vec{x}) = (1/T) \int_0^T u(\vec{x}, t) dt$ (where T is the duration of the entire season) and the transient or eddy component is defined as $u'(\vec{x}, t) = u(\vec{x}, t) - \hat{u}(\vec{x})$. Even though the tropospheric flow does not possess a clear spectral gap, i.e. there is a near continuum of active (temporal and spatial) scales, we expect the above decomposition to separate processes which vary on scales that are farthest apart [21].

Fig. 3 and Fig. 4 show the zonal and meridional LVCF's computed by exclusively utilizing the Eulerian time mean (upper panels) and Eulerian eddy fields (lower panels). In spite of the crudeness of our partition, the similarity between the eddy LVCF's in both cases is evident. Indeed, apart from the slight anticorrelation retained in the meridional eddy LVCF, both $R_{u'}(\tau)$ and $R_{v'}(\tau)$ are rapidly decaying functions with a timescale of the order of a couple of days.

On the other hand the zonal and meridional time mean LVCF's are strikingly different. Where $R_{\hat{u}}(\tau)$ is strongly correlated on long timescales - something we would expect from a slowly varying zonal jet - $R_{\hat{v}}(\tau)$ represents oscillatory motion as induced by a large scale wave. Moreover, comparing the behaviour of $R_{v'}(\tau)$ and $R_{\hat{v}}(\tau)$ leads us primarily attribute the anticorrelation observed in $R_v(\tau)$ to the time mean component of the flow. Indeed, behaviour consistent with these results has been observed in studies of balloon trajectories in the Southern Hemisphere [22] (see especially their Figs. 9, 10 and the discussion regarding the timescales involved in the definition of stationary and transient components of the flow).

III. ABSOLUTE DISPERSION

The absolute dispersion (AD) is defined as,

$$AD(t) = \langle (x(t) - x(0))^2 \rangle_S \quad (2)$$

For ideal (i.e. isotropic, homogenous, stationary and zero time mean) flows, we have [5], [2],

$$AD(t) = 4E \int_0^t R(\tau) (t - \tau) d\tau ; E = \text{kinetic energy} \quad (3)$$

The short time limit (i.e. $\tau \rightarrow 0$) of the above yields ballistic motion whereas when T_u is finite, the long time limit (i.e. $\tau \gg T_u$) yields diffusive behaviour [1]. The presence of other

exponents, i.e. $\text{AD}(t) \sim t^\gamma$; $\gamma \neq 1$, is referred to as anomalous diffusion [6]. Before displaying the results, let us fix some notation. We denote the total AD by $A(t)$, i.e. $A(t) = \langle (x(t) - x(0))^2 + (y(t) - y(0))^2 + (z(t) - z(0))^2 \rangle_S$, where x, y, z are cartesian coordinates. Further the individual components of the AD are denoted by $A_i(t)$ where i represents a coordinate, for eg. $A_x(t) = \langle (x(t) - x(0))^2 \rangle_S$.

From Eq. (3) we have $R(\tau) \sim \tau^{-\alpha} \Rightarrow \text{AD}(t) \sim t^{2-\alpha}$. Even though the non-ideal nature of the present flow, especially its rich time mean structure [3], [4], is likely to invalidate the direct applicability of Eq. (3) - nonetheless, from the form of $R_u(\tau)$ (whether one takes it to be a power law or a sum of exponentials, both being equivalent from the discussion in the previous section) it is reasonable to expect the zonal AD to exhibit anomalous behaviour at intermediate timescales. Indeed as can be seen in Fig. 5 (which shows $A_x(t)$ as computed using the daily wind data)⁴,

$$A_x(t) \sim t^2 \quad 0 < t \leq 2 \quad [\text{Ballistic}] \quad (4)$$

$$A_x(t) \sim t^\gamma \quad ; \quad \gamma = 1.45 \quad 2 < t \leq 8 \quad [\text{Anomalous : Superdiffusive}] \quad (5)$$

$$A_x(t) \sim R_e^2 \quad ; \quad R_e = \text{Earth Radius} \quad t > 8 \quad [\text{Saturation}] \quad (6)$$

In order to avoid the effective boundedness of the domain we unwrap the longitude and present $A_\lambda(t)$ in Fig. 6. Now the anomalous regime (t^δ ; $\delta = 1.6$) lasts from $T_1 < t < T_2$ days ($T_1 \sim 2$ and $T_2 \sim 25$), after which we see the beginning of an asymptotic diffusive regime (lower panel of Fig. 4)⁵. It is worth mentioning that the anomalous behaviour of $A_\lambda(t)$ is in close agreement with laboratory experiments on quasi-geostrophic flows [23]. Further, zonal superdiffusion has been identified in studies involving large amplitude Rossby waves [24] and in more general PV conserving flows (where ofcourse, the superdiffusion is along PV contours) [25]⁶.

Regarding the meridional AD, apart from the initial ballistic behaviour we expect to see normal diffusion at large t , as $R_v \rightarrow 0$ quite rapidly. Once again, we use Eq. (3) to get a feel for the meridional AD at intermediate timescales. Qualitatively approximating $R_v(\tau) \sim e^{-\tau/C_1} \cos(\omega\tau)$ (Fig. 2), numerical integration of Eq. (3) yields the AD shown in Fig. 7. Apart from the two asymptotic regimes we notice transient subdiffusive scaling. This is in accord with results utilizing random shear flows, where anticorrelation in the LCVF was associated with subdiffusion and even complete trapping in extreme cases [26]. Indeed the actual meridional AD, $A_z(t)$ shown in Fig. 8, behaves in precisely the same manner,

$$A_z(t) \sim t^2 \quad 0 < t \leq 2 \quad [\text{Ballistic}] \quad (7)$$

$$A_z(t) \sim t^{0.7} \quad 2 < t \leq 7 \quad [\text{Anomalous : Subdiffusive}] \quad (8)$$

$$A_z(t) \sim t \quad t > 7 \quad [\text{Diffusive}] \quad (9)$$

⁴ $A_y(t)$ is virtually identical to $A_x(t)$. Also, $A_z(t)$ (shown later) $\ll A_x(t)$ hence $A(t)$ also behaves in the same fashion as $A_x(t)$.

⁵Note that we should expect $\delta \neq \gamma$ as $A_\lambda(t)$ only involves changes in λ whereas $A_x(t)$ is sensitive to both λ and ϕ .

⁶I thank Referee C for providing references on particle motion in PV conserving systems.

Comparing this behaviour with the meridional AD in strictly PV conserving flows [24], [25] we see that in those cases the meridional AD is bounded whereas the violation of PV conservation at large times (i.e. greater than a week) leads to unbounded normal diffusion in the present situation. Such superdiffusive zonal and subdiffusive meridional behaviour has also been recently observed in a study of anisotropic drift-wave turbulence [27] - particularly remarkable is the similarity of the anomalous exponents in the two situations.

IV. SUMMARY

Employing daily wind data from the ECMWF, we have estimated the zonal and meridional LVCF's of the midlatitude tropospheric flow. The zonal LVCF is seen to be non-exponential in character. Physically, given that the midlatitude tropospheric flow has a rich time mean structure along with an energetic eddy field [3], [4] - this observation is not entirely unexpected. Moreover, from this perspective our examination of $R_{\hat{u}}(\tau)$ and $R_{u'}(\tau)$ serves to clarify the roles of the time mean and eddy fields respectively. Specifically, the eddy field by itself generates an almost exponential rapidly decaying LCVF whereas the time mean component - roughly a slowly varying unidirectional jet flow [21] - is seen to be strongly correlated.

Apart from decaying to zero in a relatively short time (≈ 1 week), the meridional LVCF exhibits an anticorrelation - i.e. $R_v(\tau) < 0$ before $R_v(\tau) \rightarrow 0$. We attribute this anticorrelation to the presence of large scale planetary waves - a basic consequence of PV conservation on a rotating planet. Examining $R_{v'}(\tau)$ we see that the meridional eddy LCVF is very similar to its zonal counterpart. Whereas $R_{\hat{v}}(\tau)$ - a manifestation of the large scale stationary waves - has an oscillatory character and indicates the time mean component to be primarily responsible for the above mentioned anticorrelation in $R_v(\tau)$.

As regards the AD the point that stands out is the simultaneous existence of superdiffusive and subdiffusive anomalous scaling in the zonal and meridional directions respectively. It must be stressed that we lack a quantitative relationship between the LCVF and the AD in this non-ideal situation. Nonetheless, a certain qualitative basis is provided by super- and sub-diffusive behaviour in ideal turbulent fields with enhanced (power laws or sums of exponentials depending on ones interpretation) and anticorrelated LVCF's respectively ⁷. Finally, given that similar behaviour has been observed in drift wave turbulence [27], we are led to speculate on the possible universality of this phenomenon in fields where (slow) jets and waves co-exist with (fast) eddies.

ACKNOWLEDGMENTS

Comments by Dr. R. Saravanan are gratefully acknowledged. Also, comments by all three referees led to a significant improvement in the material presented. This work was carried out at the National Center for Atmospheric Research which is sponsored by the National Science Foundation.

⁷Note that this anomalous behaviour is transient i.e., it is flanked on either side by an asymptotic regime. Even though in the present situation this behaviour is supported by the nature of the LVCF, it is worth keeping in mind that crossover effects (especially in the superdiffusive case) could play a role in determining the quantitative nature of the anomalous exponents [8].

-
- [1] Hinze, J., 1975: *Turbulence*, McGraw-Hill, 790pp.
 - [2] Monin, A. and A. Yaglom, 1971: *Statistical Fluid Mechanics. Vol. 1*, MIT Press, 769pp.
 - [3] Shepherd, T., 1987: Rossby waves and two-dimensional turbulence in a large-scale zonal jet. *Journal of Fluid Mech.*, **183**, 467-509.
 - [4] Shepherd, T., 1987: A spectral view of nonlinear fluxes and stationary- transient interaction in the atmosphere. *J. Atmos. Sci.*, **44**, 1166-1179.
 - [5] Taylor, G., 1921: Diffusion by continuous movement. *Proc. London Math. Soc.*, **20**, 196-211.
 - [6] Bouchaud, J-P. and A. Georges, 1990: Anomalous Diffusion in Disordered Media : statistical Mechanisms, Models and Physical Applications. *Physics Reports*, **195**, 127-293.
 - [7] Leoncini, X. and G. Zaslavsky, 2002: Jets, stickiness, and anomalous transport. *Physical Review E*, **65**, 046216.
 - [8] Boffetta, G., A. Celani, M. Cencini, G. Lacorata and A. Vulpiani, 2000: Nonasymptotic properties of transport and mixing. *Chaos*, **10**, 50-60.
 - [9] Gifford, F., 1982: Horizontal diffusion in the atmosphere : A Lagrangian-Dynamical theory. *Atmospheric Environment*, **16**, 505-512.
 - [10] Gifford, F., 1984: The random force theory : Application to meso- and large- scale atmospheric diffusion. *Boundary Layer Meteorology*, **30**, 159-175.
 - [11] Sawford, B., 1984: The basis for, and some limitations of, the Langevin equation in atmospheric relative dispersion modelling. *Atmospheric Environment*, **18**, 2405-2411.
 - [12] Pasquero, C., A. Provenzale and A. Babiano, 2001: Parameterization of dispersion in two-dimensional turbulence. *Journal of Fluid Mech.*, **439**, 279-303.
 - [13] Pecseli, H. and J. Trulsen, 1997: Eulerian and Lagrangian correlations in two-dimensional random geostrophic flows. *Journal of Fluid Mech.*, **338**, 249-276.
 - [14] Mordant, N., P. Metz, O. Michel and J.-F. Pinton, 2001: Measurement of Lagrangian Velocity in Fully Developed Turbulence. *Phys. Rev. Lett.*, **87**, 214501.
 - [15] Pope, S., 2000: *Turbulent Flows*, Cambridge, 771pp.
 - [16] Berglund, A., 2004: Nonexponential statistics of fluorescence photobleaching. *Journal of Chemical Physics*, **121**, 2899-2903.
 - [17] Feldmann, A. and W. Whitt, 1998: Fitting mixtures of exponentials to long-tail distributions to analyze network performance models. *Performance Evaluation*, **31**, 245-279.
 - [18] Starobinski, D. and M. Sidi, 2000: Modeling and analysis of power-tail distributions via classical tele-traffic methods. *Queueing Systems*, **36**, 243-267.
 - [19] Rhines, P., 1994: Jets. *Chaos*, **4**, 313-339.
 - [20] Pedlosky, J., 1987: *Geophysical Fluid Dynamics* Springer Verlag, 710pp.
 - [21] Blackmon, M., Y. Lee and J. Wallace, 1984: Horizontal Structure of the 500 mb Height Fluctuations with Long, Intermediate and Short Time Scales. *J. Atmos. Sci.*, **41**, 961-979.
 - [22] Morel, P. and M. Desbois, 1974: Mean 200-mb Circulation in the Southern Hemisphere Deduced from EOLE Balloon Flights. *J. Atmos. Sci.*, **31**, 394-407.
 - [23] Weeks, E., J. Urbach and H. Swinney, 1996: Anomalous diffusion on asymmetric random walks with a quasi-geostrophic flow example. *Physica D*, **97**, 291-310.
 - [24] Flierl, G., 1981: Particle Motions in Large-Amplitude Wave Fields. *Geophys. Astrophys. Fluid Dynamics*, **18**, 39-74.
 - [25] LaCasce, J.H. and K.G. Speer, 1999: Lagrangian statistics in unforced barotropic flows. *Journal of Marine Research*, **57**, 245-274.
 - [26] Elliott, F., D. Horntrop and A. Majda, 1997: Monte Carlo methods for turbulent tracers with long range and fractal random velocity fields. *Chaos*, **7**, 39-48.
 - [27] Basu, R., V. Naulin and J. Rasmussen, 2003: Particle diffusion in anisotropic turbulence. *Communications in Nonlinear Science and Numerical Simulation*, **8**, 477-492.

V. FIGURE CAPTIONS

- Figure 1 : Upper Panel : Zonal LCVF. Lower Panel : Possible power law behaviour at intermediate timescales. Though a sum of exponential processes would result in similar behaviour at intermediate scales.
- Figure 2 : Meridional LCVF : Note $R_v(\tau) < 0$ before $R_v(\tau) \rightarrow 0$.
- Figure 3 : Upper Panel : Time Mean Zonal LCVF (DJF data). Lower Panel : Eddy Zonal LCVF. Note the different timescales in the two panels. Also, by about one week the eddy correlations have almost completely died out whereas the mean flow is still strongly correlated. JJA data (not shown) behaves in a qualitatively similar manner.
- Figure 4 : Upper Panel : Time Mean Meridional LCVF (DJF data). Lower Panel : Eddy Meridional LCVF. Once again, note the different timescales in the two panels. JJA data (not shown) behaves in a qualitatively similar manner.
- Figure 5 : Zonal AD. Ballistic \rightarrow Superdiffusive \rightarrow Saturation.
- Figure 6 : Upper Panel : DJF Longitudinal AD (Ballistic \rightarrow Superdiffusive \rightarrow Diffusive). Lower Panel : $dA_\lambda(t)/dt$ Vs. t . Note $dA_\lambda(t)/dt \rightarrow \text{Const.} \Rightarrow$ normal diffusion.
- Figure 7 : Upper Panel : Synthetic LVCF $R(\tau) \sim e^{-\tau/C_1} \cos(\omega\tau)$ ($C_1 = 7, \omega = 0.3$). Lower Panel : Induced AD.
- Figure 8 : Upper Panel : Meridional AD (JJA and DJF curves have been shifted for clarity). Ballistic \rightarrow Subdiffusive \rightarrow Diffusive. Lower Panel : $A_z(t)/t \sim t \rightarrow A_z(t)/t \sim t^\beta - 1 < \beta < 0 \rightarrow A_z(t)/t \sim \text{Const.}$

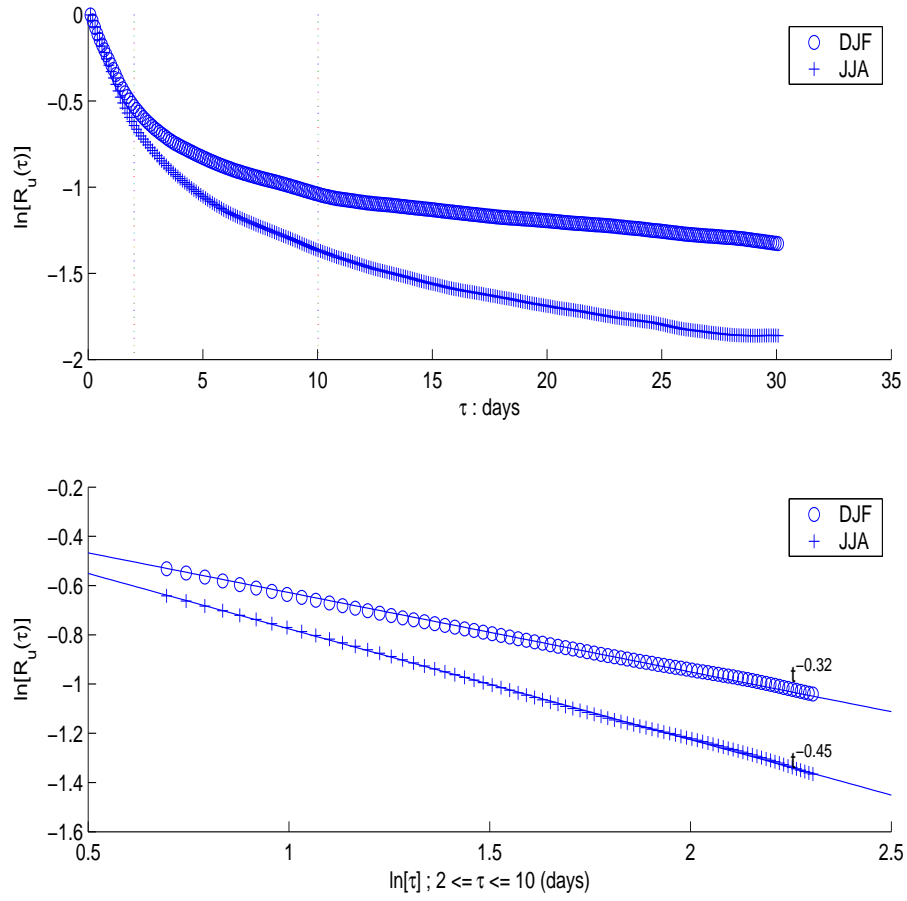


FIG. 1. Upper Panel : Zonal LCVF. Lower Panel : Possible power law behaviour at intermediate timescales. Though a sum of exponential processes would result in similar behaviour at intermediate scales.

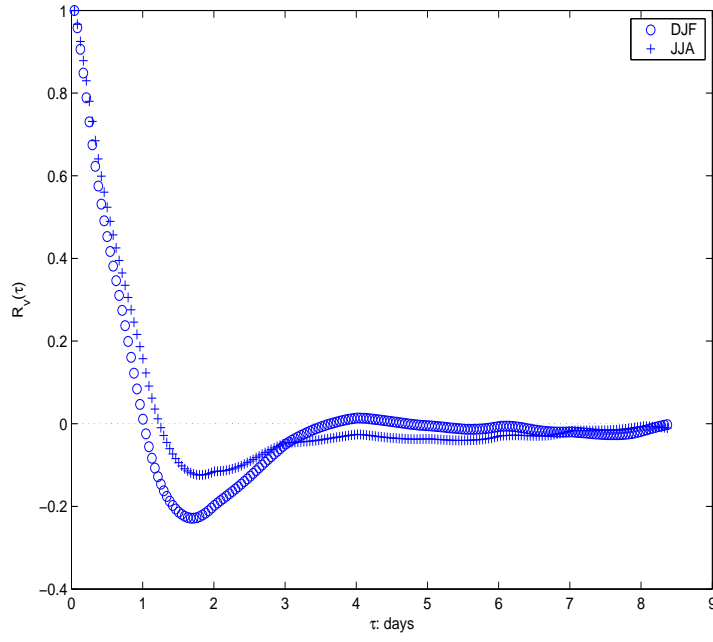


FIG. 2. Meridional LCVF : Note $R_v(\tau) < 0$ before $R_v(\tau) \rightarrow 0$.

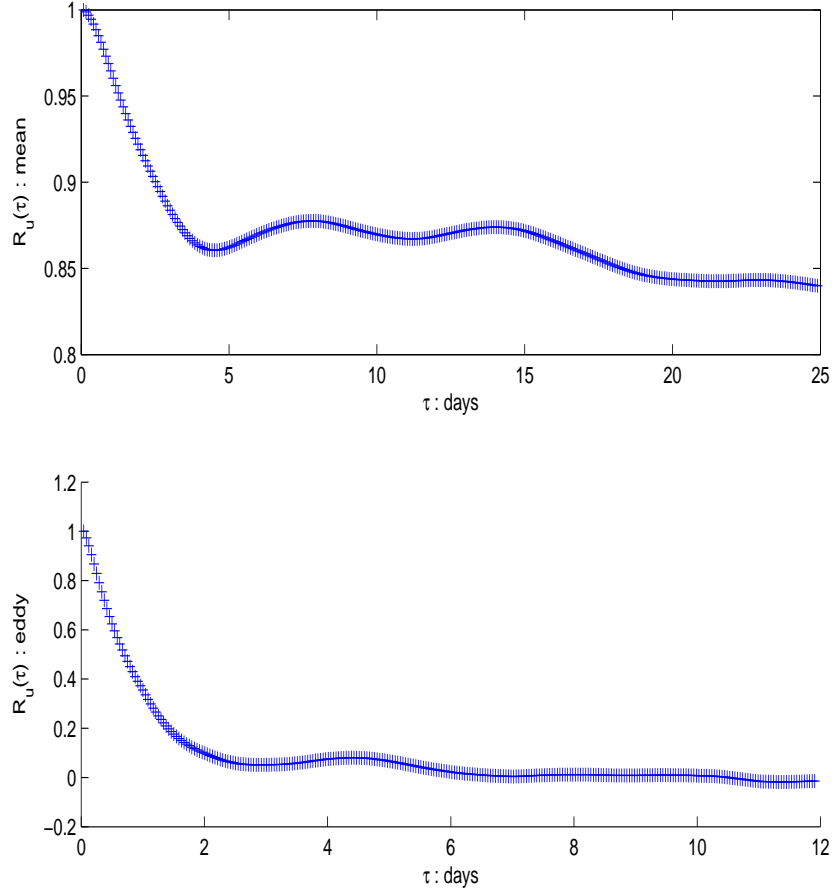


FIG. 3. Upper Panel : Time Mean Zonal LCVF (DJF data). Lower Panel : Eddy Zonal LCVF. Note the different timescales in the two panels. Also, by about one week the eddy correlations have almost completely died out whereas the mean flow is still strongly correlated. JJA data (not shown) behaves in a qualitatively similar manner.

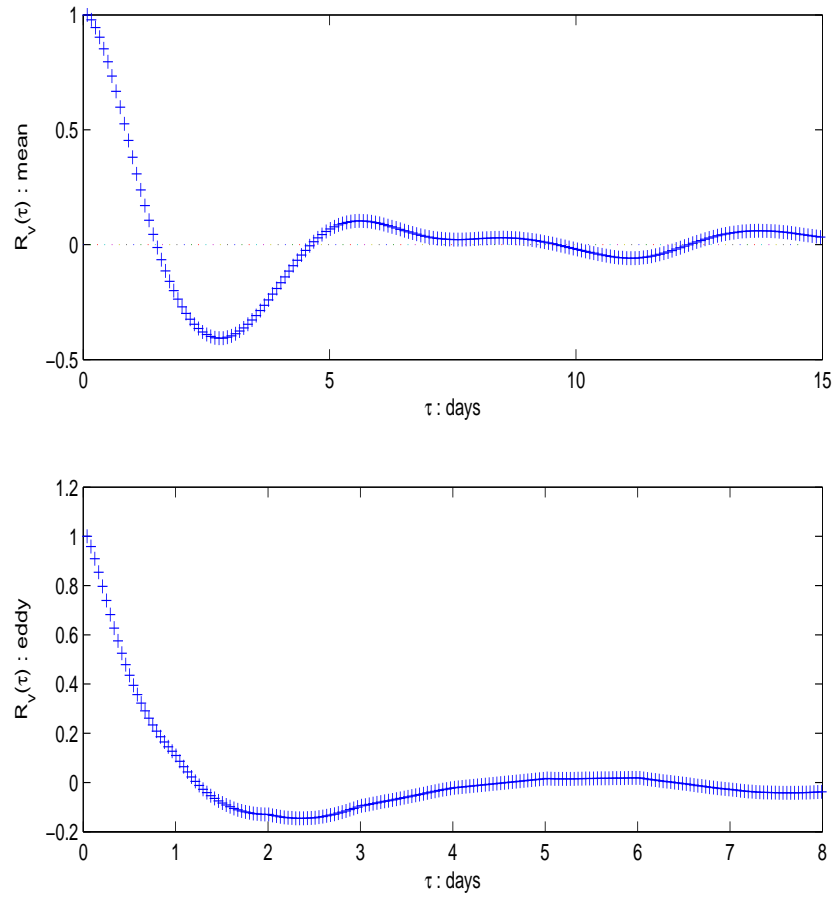


FIG. 4. Upper Panel : Time Mean Meridional LCVF (DJF data). Lower Panel : Eddy Meridional LCVF. Once again, note the different timescales in the two panels. JJA data (not shown) behaves in a qualitatively similar manner.

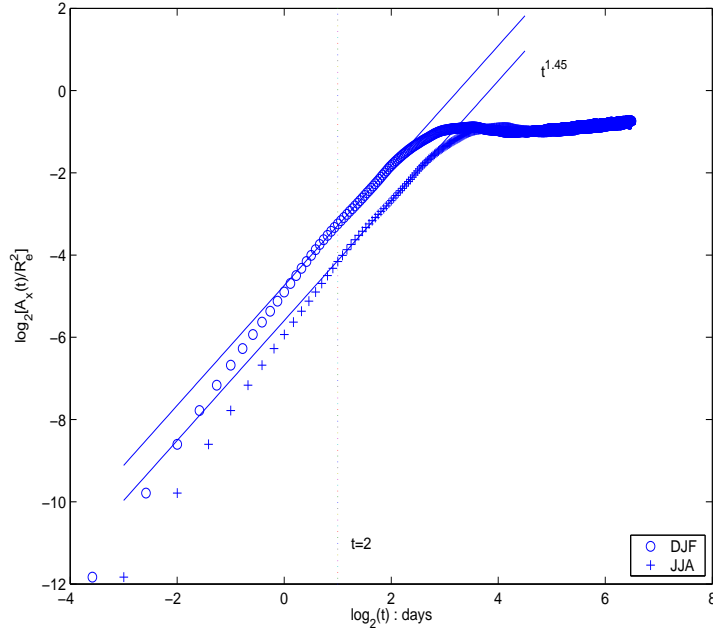


FIG. 5. Zonal AD. Ballistic \rightarrow Superdiffusive \rightarrow Saturation

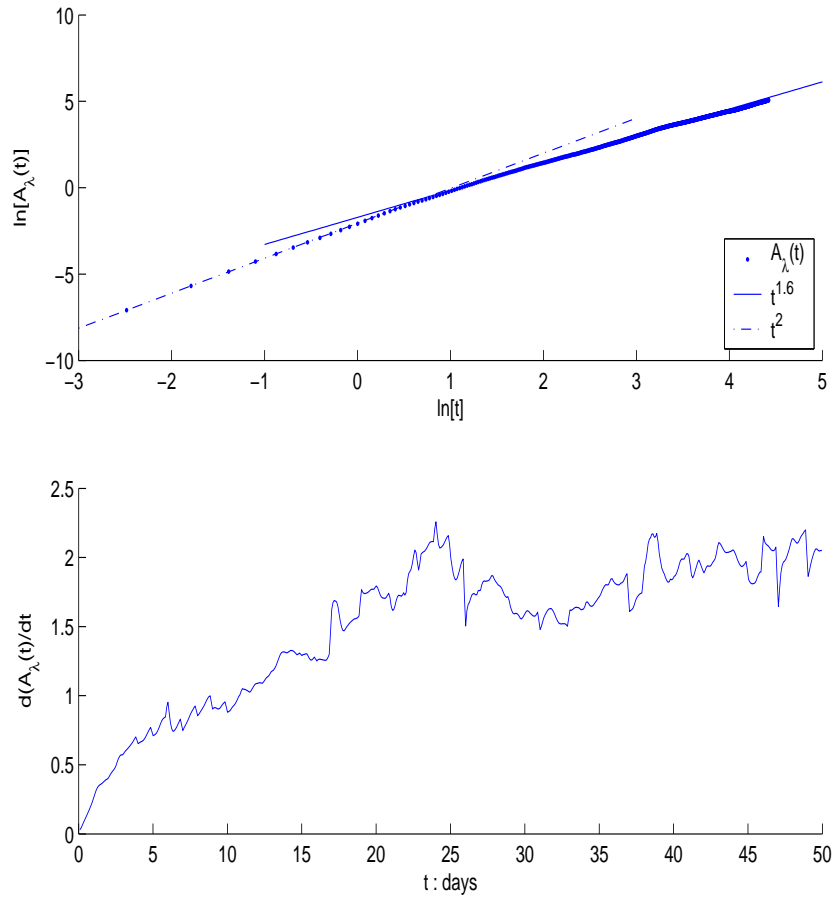


FIG. 6. Upper Panel : DJF Longitudinal AD (Ballistic \rightarrow Superdiffusive \rightarrow Diffusive). Lower Panel : $dA_\lambda(t)/dt$ Vs. t . Note $dA_\lambda(t)/dt \rightarrow \text{Const.} \Rightarrow$ normal diffusion.

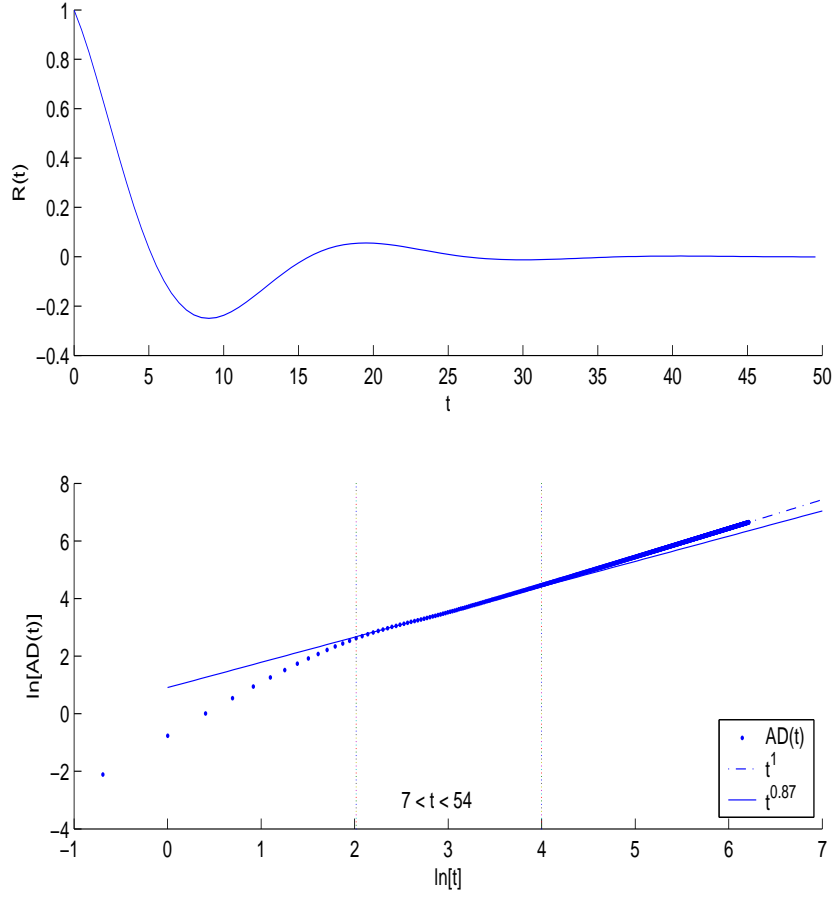


FIG. 7. Upper Panel : Synthetic LVCF $R(\tau) \sim e^{-\tau/C_1} \cos(\omega\tau)$ ($C_1 = 7, \omega = 0.3$). Lower Panel : Induced AD.

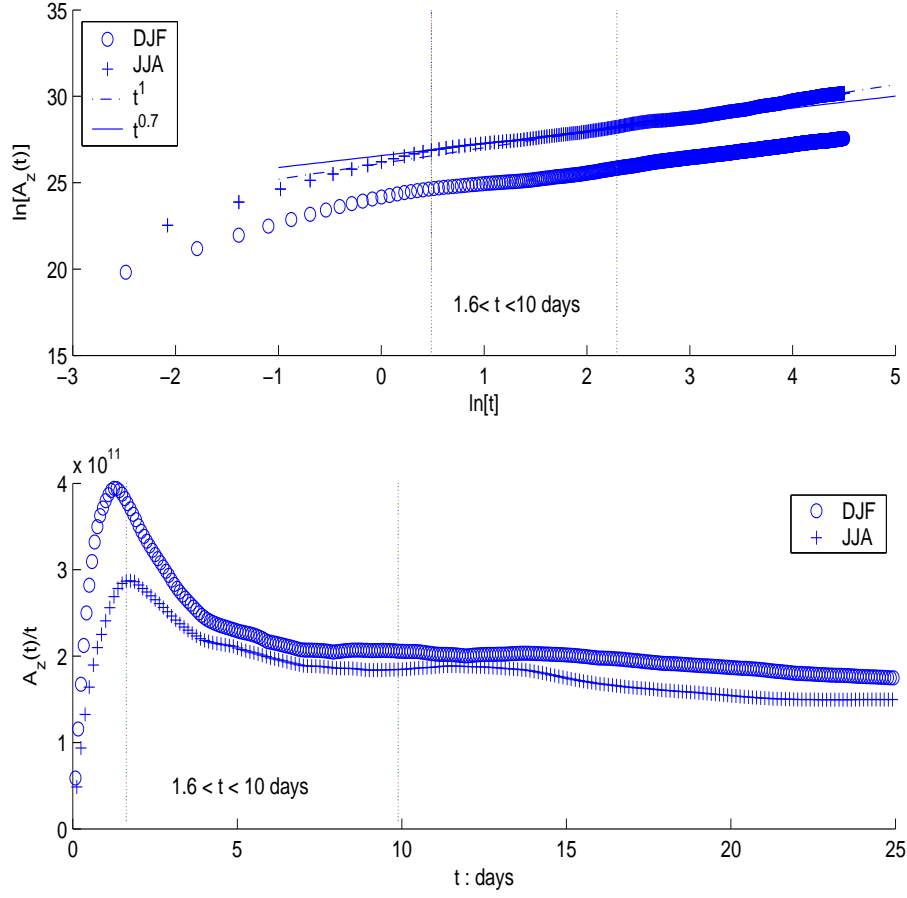


FIG. 8. Upper Panel : Meridional AD (JJA and DJF curves have been shifted for clarity). Ballistic \rightarrow Subdiffusive \rightarrow Diffusive. Lower Panel : $A_z(t)/t \sim t \rightarrow A_z(t)/t \sim t^\beta$ $-1 < \beta < 0 \rightarrow A_z(t)/t \sim \text{Const.}$